periodica polytechnica

Civil Engineering
58/3 (2014) 203–216
doi: 10.3311/PPci.7460
http://periodicapolytechnica.org/ci

RESEARCH ARTICLE

Magnetic charged system search for structural optimization

Ali Kaveh / *Ali* Zolghadr

Received 2014-04-03, accepted 2014-07-07

Abstract

In this paper the Magnetic Charged System Search algorithm is applied to structural optimization. This algorithm uses the Biot-Savar law of electromagnetism to incorporate magnetic forces into the already existing Charged System Search algorithm and thus can be considered as an extension of it. Each search agent exerts magnetic forces on other agents based on the variation of its objective function value during its last movement. This additional force provides some additional information and enhances the performance of the Charged System Search. The efficiency of the Magnetic Charged System Search is examined by application of this algorithm to four structural optimization problems. The results are compared to those of CSS and some of the methods available in the literature.

Keywords

Optimal design of structures · Charged System Search (CSS) · Magnetic Charged System Search (MCSS) · Trusses · Frames

Ali Kaveh

Centre of Excellence for Fundamental Studies in Structural Engineering, School of Civil Engineering, Iran University of Science and Technology, Narmak, P.O. Box 16846-13114, Iran
e-mail: alikaveh@iust.ac.ir

Ali Zolghadr

Centre of Excellence for Fundamental Studies in Structural Engineering, School of Civil Engineering, Iran University of Science and Technology, Narmak, P.O. Box 16846-13114, Iran

1 Introduction

Optimization algorithms can be roughly divided into two main groups consisting of mathematical programming techniques and meta-heuristic methods. Many different mathematical programming techniques have been proposed and developed during the past decades. Linear programming, convex programming, integer programming, quadratic programming, and dynamic programming are some of these approaches that have been utilized for optimization problems. These methods usually provide accurate solutions; however, most of them need the gradient information of the objective function, and are dependent on the initial points.

In order to address these shortcomings meta-heuristic algorithms are developed. These algorithms are meant to find some sub-optimal solutions in an affordable time and are usually inspired from natural phenomena. Genetic Algorithms (GA) proposed by Holland [1] and Goldberg [2] are inspired by Darwin's theory of biological evolutions. Particle Swarm Optimization (PSO) proposed by Eberhart and Kennedy [3] simulates social behavior of flocks of birds and schools of fishes. Ant Colony Optimization (ACO) formulated by Dorigo [4] imitates foraging behavior of some species of ants. Many other natural-inspired algorithms such as Simulated Annealing (SA) proposed by Kirkpatrick *et al.* [5], Harmony Search (HS) presented by Geem *et al.* [6], Gravitational Search Algorithm (GSA) proposed by Rashedi *et al.* [7], Big Bang-Big Crunch algorithm (BB-BC) proposed by Erol and Eksin [8], and improved by Kaveh and Talathari [9] have been proposed in recent years. Due to their good performance and ease of implementation, these methods have been widely applied to various problems in different fields of science and engineering. Structural optimization is one of the active branches of applications for optimization algorithms [10–18]. One of the recently developed meta-heuristic algorithms is the Charged System Search proposed by Kaveh and Talatahari [19] that uses the Coulomb and Gauss laws of physics and Newtonian laws of mechanics to guide some Charged Particles (CPs) to explore search space and locate the optimal solutions. This algorithm is further improved by utilizing the governing laws of magnetic forces and is presented as Magnetic

Charged System Search by Kaveh *et al.* [20]. In this algorithm the movements of CPs are determined due to the total force (Lorentz force) instead of using the electric forces merely as in CSS.

In this paper, the MCSS algorithm is applied to some structural optimization problems. The remainder of the paper is organized as follows: in Section 2 a brief review of the MCSS algorithm is presented. In Section 3, the formulation of the structural optimization is presented for truss and frame structures. The MCSS algorithm is then applied to different optimization problems in Section 4. Finally, some concluding remarks are provided in Section 5.

2 Optimization Algorithm

Magnetic Charged System Search (MCSS) introduced by Kaveh et al. [20] considers the optimization agents to be moving charged particles exerting a series of electric and magnetic forces on each other. These forces which are determined and controlled on the basis of the solutions' qualities and rates of progress attract the particles gradually to better positions of the search space and lead to eventual convergence.

MCSS assumes the charged particles to be moving through straight virtual wires, as shown in Fig. 1. These wires create a magnetic field on the points surrounding them depending on their radius (R), the electric current passing through them (I), and the distance to the point (r). The other CPs moving in the search space are influenced by these magnetic fields.

The steps of MCSS can be summarized as follows:

Step 1. Initialization

The initial positions of the CPs are randomly determined using a uniform source, and the initial velocities of the particles are set to zero. A memory is used to save a number of best results. This memory is called the Charged Memory (CM).

Step 2. Determination of electric and magnetic forces and the corresponding movements.

- *Electric Force Determination*: Each charged particle imposes electric forces on the other CPs according to the magnitude of its charge. The charge of each CP is:

$$q_i = \frac{fit(i) - fit_{worst}}{fit_{best} - fit_{worst}} \tag{1}$$

where $fit(i)$ is the objective function value of the ith CP, fit_{best} and fit_{worst} are the best and worst fitness values so far among all CPs, respectively.

In addition to the electric charge, the magnitudes of the electric forces exerted on the CPs are dependent on the separation distance that is,

$$r_{ij} = \frac{\left\|\mathbf{X}_i - \mathbf{X}_j\right\|}{\left\|\left(\mathbf{X}_i + \mathbf{X}_j\right)/2 - \mathbf{X}_{best}\right\| + \varepsilon} \tag{2}$$

where $\mathbf{X}_i$ and $\mathbf{X}_j$ are the positions of the ith and jth CPs, and r_{ij} is the separation distance of them. $\mathbf{X}_{best}$ is the position of the best current CP, and ε is a small positive number to prevent singularity.

The probability of the ith CP being attracted by the jth CP is expressed as:

$$p_{ij} = \begin{cases} 1 \Leftrightarrow \frac{fit(i)-fit_{best}}{fit(j)-fit(i)} > rand,\ or,\ fit(j) > fit(i) \\ 0 \Leftrightarrow else. \end{cases} \tag{3}$$

The electric resultant force $\mathbf{F}_{E,j}$, acting on the jth CP can be calculated by superposing the electric forces exerted by different CPs using the following equation,

$$\mathbf{F}_{E,j} = q_j \sum_{i,i\neq j} \left(\frac{q_i}{R^3} r_{ij} \cdot w_1 + \frac{q_i}{r_{ij}^2} \cdot w_2 \right) \cdot p_{ji} \cdot \left(\mathbf{X}_i - \mathbf{X}_j\right),$$
$$\begin{cases} w_1 = 1,\ w_2 = 0 \Leftrightarrow r_{ij} < R \\ w_1 = 0,\ w_2 = 1 \Leftrightarrow r_{ij} \geq R \end{cases} \tag{4}$$
$$j = 1, 2, ..., N$$

in which R is the radius of the particles usually taken as unity.

- *Magnetic Force Determination*: Each CP moves in a virtual wire and produces a magnetic field around itself. The average electric current of the ith CP in its kth iteration can be calculated as:

$$\left(I_{avg}\right)_{ik} = sign\left(df_{i,k}\right) \times \frac{\left|df_{i,k}\right| - df_{min,k}}{df_{max,k} - df_{min,k}} \tag{5}$$

$$df_{i,k} = fit_k(i) - fit_{k-1}(i) \tag{6}$$

where $df_{i,k}$ is the variation of the objective function in the kth movement (iteration). $fit_k(i)$ and $fit_{k-1}(i)$ are the values of the objective function of the ith CP at the start of the kth and $k-1$th iterations, respectively.

The value of the magnetic force $\mathbf{F}_{\mathbf{B},ji}$ exerted on the jth CP because of the magnetic field produced by the ith virtual wire can be expressed as:

$$\mathbf{F}_{\mathbf{B},ji} = q_j \cdot \left(\frac{I_i}{R^2} r_{ij} \cdot z_1 + \frac{I_i}{r_{ij}} \cdot z_2 \right) \cdot pm_{ji} \cdot \left(\mathbf{X}_i - \mathbf{X}_j\right),$$
$$\begin{cases} z_1 = 1,\ z_2 = 0 \Leftrightarrow r_{ij} < R \\ z_1 = 0,\ z_2 = 1 \Leftrightarrow r_{ij} \geq R \end{cases} \tag{7}$$

where q_i is the charge of the ith CP, R is the radius of the virtual wires, I_i is the average electric current in each wire, and pm_{ji} is the probability of the magnetic influence (attraction or repulsion) of the ith wire on the jth CP. This term can be computed by the following expression:

$$pm_{ji} = \begin{cases} 1 \Leftrightarrow fit(i) > fit(j) \\ 0 \Leftrightarrow else \end{cases} \tag{8}$$

This expression indicates that only a good CP can affect a bad CP by the magnetic force.

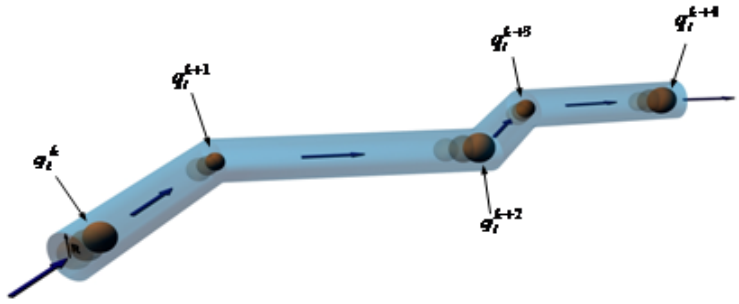

Fig. 1. A schematic view of virtual wire (movement path of a CP), q_i^k is the charge of ith CP at the end of the kth iteration (Kaveh et al. [20]).

The resultant magnetic force due to the group of CPs is then calculated as:

$$\mathbf{F}_{\mathbf{B},j} = q_j \cdot \sum_{i,i\neq j}\left(\frac{I_i}{R^2} r_{ij} \cdot z_1 + \frac{I_i}{r_{ij}} \cdot z_2\right) \cdot pm_{ji} \cdot \left(\mathbf{X}_i - \mathbf{X}_j\right),$$
$$\begin{cases} z_1 = 1,\ z_2 = 0 \Leftrightarrow r_{ij} < R \\ z_1 = 0,\ z_2 = 1 \Leftrightarrow r_{ij} \geq R \\ j = 1, 2, ..., N \end{cases} \quad (9)$$

- *Total Acting Force*: the total acting force on the jth CP due to the simultaneous effect of electric and magnetic forces is then evaluated as:

$$\sum \mathbf{F}_j = \mathbf{F}_{B,j} + \mathbf{F}_{E,j} \quad (10)$$

where $\mathbf{F_j}$ is the total force acting on the jth CP.

- *Movement Calculation*. Under the influence of the abovementioned forces, each CP moves to its new position:

$$\mathbf{X}_{j,new} = rand_{j\,1} \cdot k_a \cdot \frac{\mathbf{F}_j}{m_j} \cdot \Delta t^2 + \\ + rand_{j\,2} \cdot k_v \cdot \mathbf{V}_{j,old} \cdot \Delta t + \mathbf{X}_{j,old}, \quad (11)$$

$$\mathbf{V}_{j,new} = \frac{\mathbf{X}_{j,new} - \mathbf{X}_{j,old}}{\Delta t} \quad (12)$$

where $rand_{j1}$ and $rand_{j2}$ are two random numbers, which are uniformly distributed in the range (0,1). k_a is the acceleration coefficient, k_v is the velocity coefficient, and m_j is the mass of the particle which is considered to be equal to q_j. The velocity coefficient controls the influence of the previous velocity of the particles. In other words, this coefficient is related to the exploration ability of the algorithm. The acceleration coefficient controls the effect of the acting force i.e. it influences the exploitation tendency of the algorithm. In order to maintain more exploration at the early iterations and more exploitation at the final iterations the magnitudes of k_a and k_v are set as:

$$k_a = 0.5(1 + iter/iter_{\max}), \ldots k_v = 0.5(1 - iter/iter_{\max}) \quad (13)$$

where $iter$ is the current iteration number, and $iter_{max}$ is the maximum number of iterations. Therefore, the value for k_a increases as the optimization process proceeds, while the value for k_v decreases.

Step 3. Charged Memory (CM) Updating

At the end of each iteration the Charged Memory is updated i.e. less good particles stored in previous iterations are discarded and better newly found particles are stored.

Step 4. Checking the Termination Criteria

Steps 2 and 3 are repeated until one of the specified termination criteria is satisfied.

3 Problem formulation

3.1 Truss optimization problem

In a truss optimization problem the goal is to minimize the weight of the structure while satisfying some constraints. These constraints can be imposed on stresses in members, displacements of nodes, natural frequencies and other response parameters. Cross-sectional areas of the members are considered to be the design variables which can be assumed to change either continuously or discretely. The optimization problem can be stated mathematically as follows:

$$\begin{aligned} &\text{Find } X = [x_1, x_2, x_3, \ldots, x_n] \\ &\text{to minimize } \ Mer(X) = f(X) \times f_{penalty}(X) \\ &\text{Subject to:} \\ &\sigma_{i\min} \leq \sigma_{i\,l} \leq \sigma_{i\max} \\ &\delta_{k\min} \leq \delta_{k\,l} \leq \delta_{k\max} \\ &\omega_m \leq \omega_m^* \ \text{ for some natural frequencies } \ m \\ &\omega_n \geq \omega_n^* \ \text{ for some natural frequencies } \ n \\ &i = 1, 2, \ldots, nm; k = 1, 2, \ldots, nn; l = 1, 2, \ldots, lc; \end{aligned} \quad (14)$$

where X is the vector containing the design variables; nm and nn are the number of members and nodes of structure, respectively; lc is the number of loading conditions; n is the number of variables which is chosen with respect to symmetry and practice requirements; $Mer(X)$ is the merit function; $f(X)$ is

the cost function, which is taken as the weight of the structure; $f_{penalty}(X)$ is the penalty function which is taken as zero when all of the constraints are satisfied; dc is the number of displacement constraints; σ_i is the stress of the ith member and $\sigma_{i\ min}$ and $\sigma_{i\ max}$ are its lower and upper bounds, respectively; δ_j is the displacement of the jth degree of freedom and $\delta_{k\ min}$ and $\delta_{k\ max}$ are the corresponding lower and upper limits, respectively; ω_m is the mth natural frequency of the structure and ω_m^* is its upper bound. ω_n is the nth natural frequency of the structure and ω_n^* is its lower bound.

The constraints are handled using a penalty function approach. The penalty function can be defined as:

$$F_{penalty}(A) = (1 + \varepsilon_1 \cdot v)^{\varepsilon_2}, v = \sum_{i=1}^{q} v_i \tag{15}$$

where q is the number of constraints. If the ith constraint is satisfied v_i will be taken as zero, if not it will be taken as:

$$v_i = \left| 1 - \left(\frac{p_i}{p_i^*} \right) \right| \tag{16}$$

where p_i is the response of the structure and p_i^* is its bound. The parameters ε_1 and ε_2 are parameters to the exploration and the exploitation rate of the search process.

3.2 Frame optimization problem

Optimal design of frame structures can be mathematically formulated as:

$$\begin{aligned}
&\text{Find } X = [x_1, x_2, x_3, \ldots, x_n] \\
&\text{to minimizes } Mer(X) = f(X) \times f_{penalty}(X) \\
&\text{subjected to:} \\
&v_i^{\sigma} = \left| \frac{\sigma_i}{\sigma_i^a} \right| - 1 \geq 0 \quad i = 1, 2, \ldots, nm \quad \text{for stress constraints} \\
&v^{\Delta} = \frac{\Delta}{H} - R \geq 0 \quad \text{for maximum lateral displacement} \\
&v_j^d = \frac{d_j}{h_j} - Rj \geq 0 \quad i = 1, 2, \ldots, ns \\
&\text{for inter-story drift constraints}
\end{aligned} \tag{17}$$

Here σ_I is stress in ith element; σ_i^a is the allowable stress in ith member; nm is the number of frame members in the structure; Δ is the maximum lateral displacement; H is the height of the structure; R is the maximum drift index; d_j is the inter-story drift; h_j is the story height of the jth floor; ns is the total number of stories; and R_j is the inter-story drift index permitted by the code of practice.

AISC 2001 [21] is used here for the design of frame structures. The maximum allowable inter-story drift index is taken as 1/300 and for the LRFD interaction formula (AISC 2001, Equation H1-1a, b), the constrains are defined as:

$$\begin{aligned}
&v^I = \frac{P_u}{2\varphi_c P_n} + \left(\frac{M_{ux}}{\varphi_b M_{nx}} + \frac{M_{uy}}{\varphi_b M_{ny}} \right) - 1 \geq 0 \\
&for\ \frac{P_u}{\varphi_c P_n} < 0.2
\end{aligned} \tag{18}$$

$$\begin{aligned}
&v^I = \frac{P_u}{\varphi_c P_n} + \frac{8}{9} \left(\frac{M_{ux}}{\varphi_b M_{nx}} + \frac{M_{uy}}{\varphi_b M_{ny}} \right) - 1 \geq 0 \\
&for\ \frac{P_u}{\varphi_c P_n} \geq 0.2
\end{aligned} \tag{19}$$

where P_u is the required axial strength (tension or compression); P_n is the nominal axial strength (tension or compression); φ_c is the resistance factor ($\varphi_c = 0.9$ for tension and $\varphi_c = 0.85$ for compression); M_{ux} and M_{uy} are the required flexural strengths in the x and y directions, respectively; M_{nx} and M_{ny} are the nominal flexural strengths in the x and y directions (for two-dimensional structures, $M_{ny} = 0$); and φ_b is the flexural resistance reduction factor ($\varphi_b = 0.9$).

The same penalty function as used in truss optimization can be used here.

4 Numerical Examples

Four numerical examples consisting of both frames and trusses with different performance constraints are considered here:

- A ten-bar truss with frequency constraints
- A 72-bar spatial truss with stress and displacement constraints
- A one-bay eight-story frame with lateral drift constraint
- A three-bay 24-story frame with LRFD specification and inter-story drift constraints

A population of 25 CPs is considered for the first three examples and 50 CPs are used for the last one. Maximum number of iterations is considered as the termination criterion. The optimal results obtained from the proposed algorithm are compared to some of the previously reported results. These comparisons indicate the viability of the algorithm in solving different types of structural optimization problems.

In order to calculate the effective length factors which are needed in example 4 the following approximate formula based on Dumonteil [22] is used:

$$K = \sqrt{\frac{1.6\, G_A G_B + 4\,(G_A + G_B) + 7.5}{G_A + G_B + 7.5}} \tag{20}$$

where G_A and G_B refer to the stiffness ratio or the relative stiffness of a column at its two ends.

Example 1: A ten-bar truss

Frequency constraint size optimization of a 10-bar planar truss as shown in Fig. 2 is considered as the first example.

This example is viewed as one of the most well-known benchmark problems in frequency constraint structural optimization. Each member's cross-sectional area is regarded as an independent continuous variable. A non-structural mass of 454.0 kg is attached to the free nodes. Table 1 shows the material properties, variable bounds, and frequency constraints for this example. This problem has been investigated by Grandhi and Venkayya [23] using the optimality algorithm. Sedaghati, *et al.* [24] have solved it by sequential quadratic programming and the finite element force method. Wang et al. [25] have used an evolutionary node shift method and Lingyun et al. [26] have used a niche hybrid genetic algorithm to optimize this structure. Gomes [27] has analyzed this problem using the particle swarm algorithm. Kaveh and Zolghadr have investigated the problem using the standard and an enhanced CSS [28] and a hybridized CSS-BBBC algorithm with trap recognition capability [29].

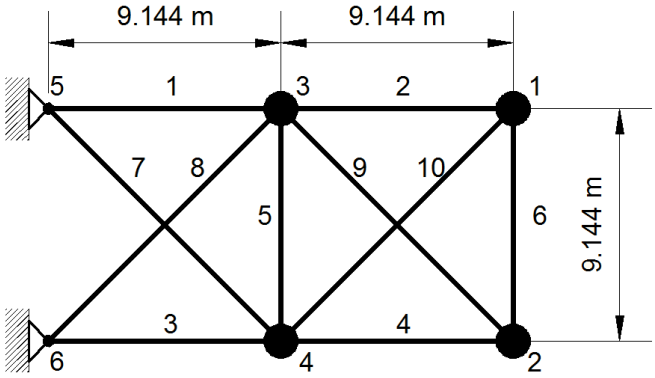

Fig. 2. A ten-bar planar truss with masses shown in bigger solid circles

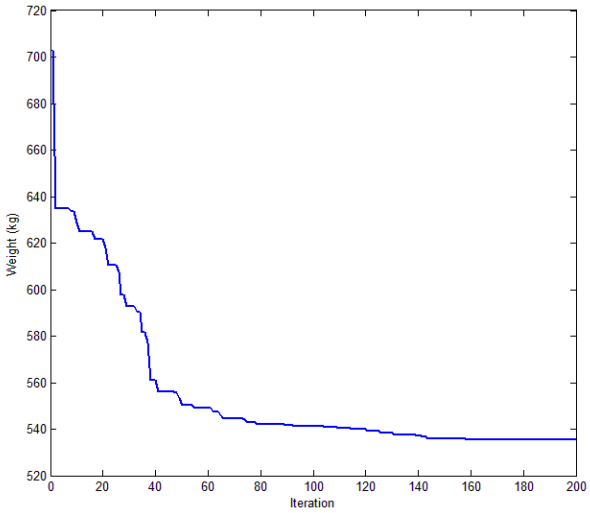

Fig. 3. Convergence curve of the best run for the 10-bar planar truss

Table 2 shows the optimal solutions found by different algorithms. It should be noted that a modulus of elasticity of $E = 6.98 \times 10^{10}$ Pa is used in Gomes [27] and Kaveh and Zolghadr [23, 24]. This will generally result in relatively lighter structures. Considering this, it appears that the proposed algorithm has obtained one of the best solutions so far. Using $E = 6.98 \times 10^{10}$ Pa the proposd algorithm finds a structure weighted 529.11 kg, which is lighter than that of CSS and enhanced CSS and is only slightly heavier than CSS-BBBC.

Table 3 presents the natural frequencies of the optimized structures obtained by different methods. All of the constraints are satisfied according to the table with an exception of the structure found by Sedaghati *et al.* [24]

The convergence curve of the best run of the MCSS optimizing the 10-bar planar truss is depicted in Fig. 3.

Example 2: A 72-bar spatial truss

A 72-bar space truss as shown in Fig. 4 is considered as the second example. This problem has been studied previously by Wu and Chow [30], Li et al [31] and Kaveh and Talatahari [32] among others. The material density is 0.1 lb/in^3 (2767.990 kg/m^3) and the modulus of elasticity is 10,000 ksi (68,950 MPa). The members are subjected to stress limitations of ±25 ksi (±172.375 MPa). The uppermost nodes are subjected to displacement limitations of ±0.25 in (±0.635 cm) both in x and y directions. The discrete variables are selected from Table 4. The loading conditions applied to the structure are listed in Table 5. The elements of this structure are grouped in 16 groups according to Table 6.

Optimal results obtained by different methods are listed in Table 7. It can be seen that the MCSS algorithm has obtained the best results. Fig. 5 represents the convergence curve of the best run of MCSS for the 72-bar spatial truss.

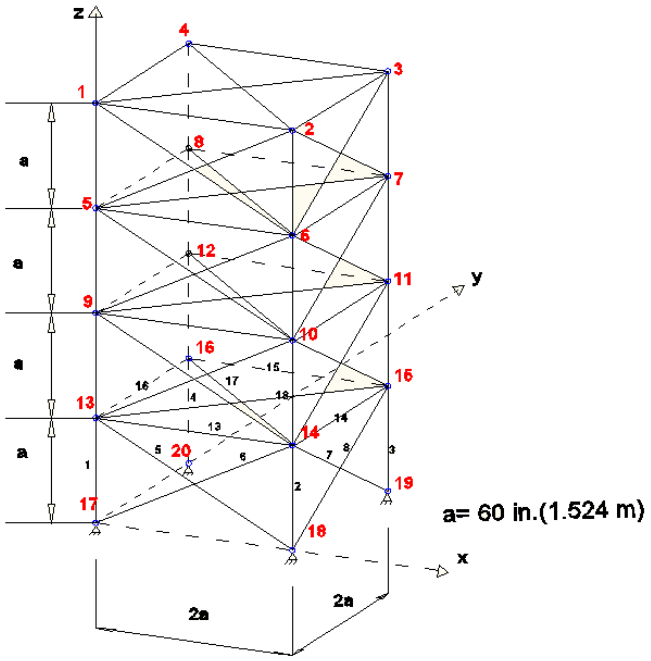

Fig. 4. Node and element numbering scheme for the 72-bar spatial truss

Tab. 1. Material properties, variable bounds and frequency constraints for the 10-bar truss structure

Property/unite	Value
E (Modulus of elasticity)/ N/m^2	6.89 ×10^{10}
ρ (Material density)/ kg/m^3	2770.0
Added mass/ kg	454.0
Design variable lower bound/ m^2	0.645 ×10^{-4}
L (Main bar's dimension)/ m	9.144
Constraints on first three frequencies/ Hz	$\omega_1 \geq 7$, $\omega_2 \geq 15$, $\omega_3 \geq 20$

Tab. 2. Optimal design cross sections (cm^2) for several methods for the ten bar planar truss (weight does not include added masses).

Element number	Grandhi and Venkayya [23]	Sedaghati et al. [24]	Wang et al. [25]	Lingyun et al. [26]	Gomes [27]	Kaveh and Zolghadr			Present work
						Standard CSS [28]	Enhanced CSS [28]	CSS-BBBC [29]	
1	36.584	38.245	32.456	42.23	37.712	38.811	39.569	35.274	37.727
2	24.658	9.916	16.577	18.555	9.959	9.0307	16.740	15.463	14.216
3	36.584	38.619	32.456	38.851	40.265	37.099	34.361	32.11	35.206
4	24.658	18.232	16.577	11.222	16.788	18.479	12.994	14.065	16.413
5	4.167	4.419	2.115	4.783	11.576	4.479	0.645	0.645	0.657
6	2.070	4.419	4.467	4.451	3.955	4.205	4.802	4.880	4.639
7	27.032	20.097	22.810	21.049	25.308	20.842	26.182	24.046	22.246
8	27.032	24.097	22.810	20.949	21.613	23.023	21.260	24.340	25.447
9	10.346	13.890	17.490	10.257	11.576	13.763	11.766	13.343	10.822
10	10.346	11.452	17.490	14.342	11.186	11.414	11.392	13.543	13.953
Weight (kg)	594.0	537.01	553.8	542.75	537.98	531.95	529.25	529.09	535.31

Tab. 3. Natural frequencies (Hz) of the optimized structures (the ten-bar planar truss)

Frequency number	Grandhi and Venkayya [23]	Sedaghati et al. [24]	Wang et al. [25]	Lingyun et al. [26]	Gomes [27]	Kaveh and Zolghadr			Present work
						Standard CSS [28]	Enhanced CSS [28]	CSS-BBBC [29]	
1	7.059	6.992	7.011	7.008	7.000	7.000	7.000	7.000	7.000
2	15.895	17.599	17.302	18.148	17.786	17.442	16.238	16.119	16.244
3	20.425	19.973	20.001	20.000	20.000	20.031	20.000	20.075	20.002
4	21.528	19.977	20.100	20.508	20.063	20.208	20.361	20.457	20.066
5	28.978	28. 173	30.869	27.797	27.776	28.261	28.121	29.149	27.796
6	30.189	31.029	32.666	31.281	30.939	31.139	28.610	29.761	29.520
7	54.286	47.628	48.282	48.304	47.297	47.704	48.390	47.950	48.994
8	56.546	52.292	52.306	53.306	52.286	52.420	52.291	51.215	51.492

Tab. 4. The available cross-sectional areas of the ASIC 1989 code [33].

No.	in^2	mm^2	No.	in^2	mm^2
1	0.111	71.613	33	3.840	2477.423
2	0.141	90.96786	34	3.870	2496.778
3	0.196	126.4518	35	3.880	2503.229
4	0.250	161.2905	36	4.180	2696.778
5	0.307	198.0648	37	4.220	2722.584
6	0.391	252.2584	38	4.490	2896.778
7	0.442	285.1617	39	4.590	2961.294
8	0.563	363.2263	40	4.800	3096.778
9	0.602	388.3876	41	4.970	3206.456
10	0.766	494.1942	42	5.120	3303.23
11	0.785	506.4523	43	5.740	3703.231
12	0.994	641.2912	44	7.220	4658.071
13	1.000	645.1622	45	7.970	5141.942
14	1.228	792.2591	46	8.530	5503.233
15	1.266	816.7753	47	9.300	6000.008
16	1.457	940.0013	48	10.850	7000.009
17	1.563	1008.388	49	11.500	7419.365
18	1.620	1045.163	50	13.500	8709.689
19	1.800	1161.292	51	13.900	8967.754
20	1.990	1283.873	52	14.200	9161.303
21	2.130	1374.195	53	15.500	10000.01
22	2.380	1535.486	54	16.000	10322.59
23	2.620	1690.325	55	16.900	10903.24
24	2.630	1696.776	56	18.800	12129.05
25	2.880	1858.067	57	19.900	12838.73
26	2.930	1890.325	58	22.000	14193.57
27	3.090	1993.551	59	22.900	14774.21
28	1.130	729.0332	60	24.500	15806.47
29	3.380	2180.648	61	26.500	17096.8
30	3.470	2238.713	62	28.000	18064.54
31	3.550	2290.326	63	30.000	19354.86
32	3.630	2341.939	64	33.500	21612.93

Tab. 5. Loading conditions for the 72-bar space truss.

node	Case 1			Case 2		
	Px kips (kN)	Py kips (kN)	Pz kips (kN)	Px kips(kN)	Py kips(kN)	Pz kips (kN)
1	0.5(-22.25)	0.5(22.25)	-0.5(-22.25)	_	_	-0.5(-22.25)
2	_	_	_	_	_	-0.5(-22.25)
3	_	_	_	_	_	-0.5(-22.25)
4	_	_	_	_	_	-0.5(-22.25)

Tab. 6. Element grouping for the 72-bar truss.

Group number	Elements	Group number	Elements
1	A1–A4	9	A37–A40
2	A5–A12	10	A41–A48
3	A13–A16	11	A49–A52
4	A17–A18	12	A53–A54
5	A19–A22	13	A55–A58
6	A23–A30	14	A59–A66
7	A31–A34	15	A67–A70
8	A35–A36	16	A71–A72

Tab. 7. Comparison of optimal designs for the 72-bar spatial truss structure

Variables (in^2)	Wu and Chow [30]	Li et al. [31]	Kaveh and Talatahari [32]	Present work in^2 (cm^2)	
				CSS	MCSS
1	0.196	4.97	1.800	0.141 (0.91)	0.141 (0.91)
2	0.602	1.228	0.442	0.391 (2.52)	0.391 (2.52)
3	0.307	0.111	0.141	0.196 (1.26)	0.196 (1.26)
4	0.766	0.111	0.111	0.563 (3.63)	0.442 (2.85)
5	0.391	2.880	1.228	0.250 (1.61)	0.307 (1.98)
6	0.391	1.457	0.563	0.307 (1.98)	0.307 (1.98)
7	0.141	0.141	0.111	0.111 (0.72)	0.111 (0.72)
8	0.111	0.111	0.111	0.111 (0.72)	0.111 (0.72)
9	1.800	1.563	0.563	1.228 (7.92)	1.266 (8.17)
10	0.602	1.228	0.563	0.391 (2.52)	0.307 (1.98)
11	0.141	0.111	0.111	0.111 (0.72)	0.111 (0.72)
12	0.307	0.196	0.250	0.111 (0.72)	0.111 (0.72)
13	1.563	0.391	0.196	1.563 (10.08)	1.99 (12.84)
14	0.766	1.457	0.563	0.307 (1.98)	0.307 (1.98)
15	0.141	0.766	0.442	0.111 (0.72)	0.111 (0.72)
16	0.111	1.563	0.563	0.111 (0.72)	0.111 (0.72)
Weight (lb)	427.203	933.09	393.380	391.063 (176.95kg)	388.936 (175.99 kg)

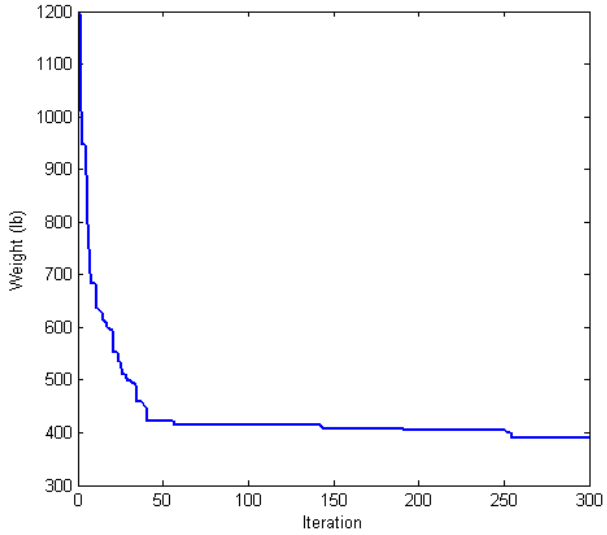

Fig. 5. Convergence curve of the best run for the 72-bar spatial truss

According to Table 7, MCSS obtains the lightest structure among the present methods. For further comparison, the problem is also solved using the standard CSS. It can be seen that the MCSS performs slightly better than the standard CSS.

Example 3: A one-bay eight-story frame

Configuration and the applied loads of a one-bay eight-story frame are depicted in Fig. 6. Several researchers have optimized this structure using different optimization approaches. Khot et al. [34] used an optimality criterion to investigate it. Camp et al. [35] optimized it using a Genetic algorithm and Kaveh and Shojaee [36] and Kaveh and Talatahari [37] utilized ACO and IACO to solve it.

The 24 elements of the structure are grouped into 8 design variables; the same beam section to be used for two consecutive stories, beginning at the foundation, and that the same column section is used every two consecutive stories. The only performance constraint is considered to be the structure's lateral drift at the top story (no more than 5.08 cm). The modulus of elasticity of the material used is taken as $E = 200$ GPa. All frame sections are chosen from the entire set of 267 W-shapes.

Table 8 presents a comparison between the best results obtained by different methods for the one-bay eight-story frame. Fig. 7 shows the convergence curve of the best run for the one-bay eight-story frame.

Table 8 indicates that the present algorithm has obtained the best result for this example. Comparison of the results shows that the performance of MCSS is better than that of CSS.

Example 4: A 3-bay 24-story frame

Topology and applied loads of a 3-bay 24-story frame are depicted in Fig. 8. This structure has been designed originally by Davison and Adams [38]. Saka and Kameshki [39] utilized a GA algorithm to obtain a least-weight design conforming to AISC specifications [23] and to BS 5950 [40]. Camp et al. [41] utilized ACO conforming to AISC specifications [23]. Kaveh

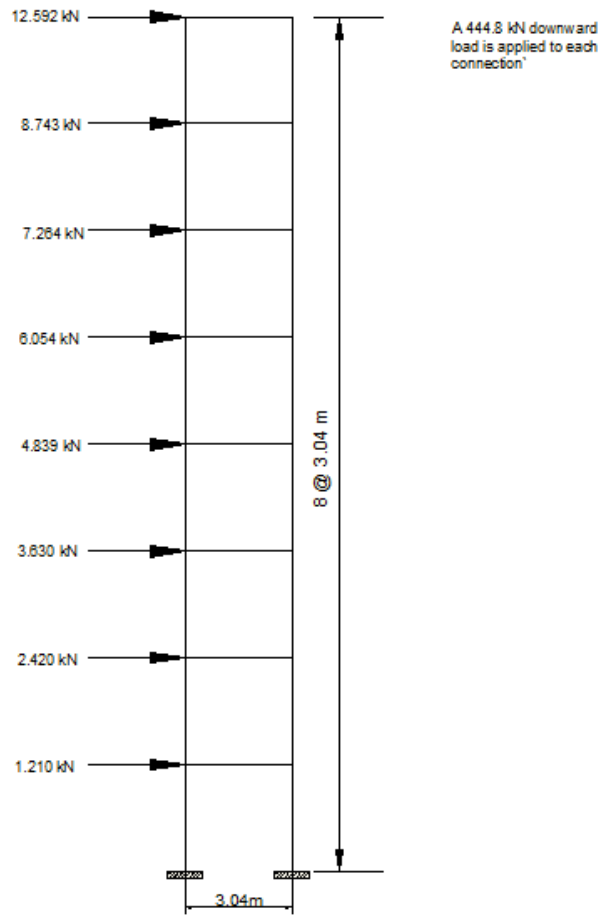

Fig. 6. A one-bay eight-story frame

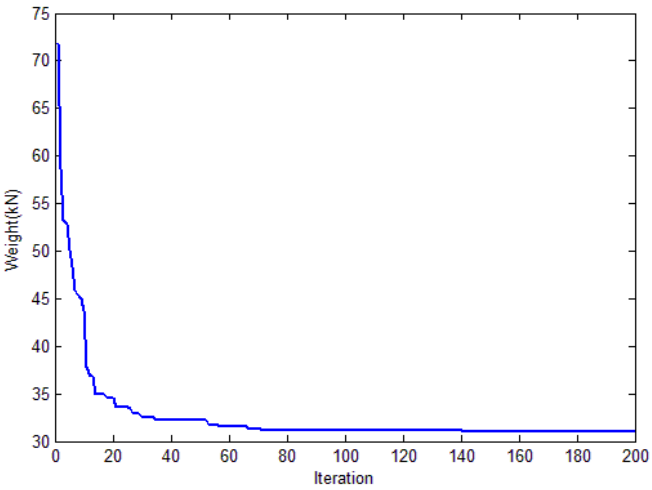

Fig. 7. Convergence curve of the best run for the one-bay eight-story frame

and Talatahari [37] used an improved ACO to develop a design conforming to the LRFD specification (AISC 2001) and used an inter-story drift displacement constraint. Kaveh and Talatahari [42] utilized standard CSS to optimize the structure using the same constraints. Here LRFD interaction formula (AISC 2001) together with inter-story drift is considered as performance constraints. The modulus of elasticity of the material is taken as $E = 205$ GPa and it's yield stress as $f_y = 230.3$ MPa.

Tab. 8. Comparison of the best results for the one-bay eight-story frame

Element group no.	AISC W-shapes						
	Element group	Khot et al. [34]	Camp et al. [35]	Kaveh and Shojaee [36]	Kaveh and Talatahari [37]	Proposed algorithm	
						CSS	MCSS
1	Beam 1-2S	W21X68	W18X35	W16X26	W21X44	W21X44	W16X31
2	Beam 3-4S	W24X55	W18X35	W18X40	W18X35	W16X31	W18X35
3	Beam 5-6S	W21X50	W18X35	W18X35	W18X35	W16X26	W16X26
4	Beam 7-8S	W12X40	W18X26	W12X22	W12X22	W16X26	W16X26
5	Column 1-2S	W14X34	W18X46	W18X40	W18X40	W18X40	W21X44
6	Column 3-4S	W10X 39	W16X31	W16X26	W16X26	W14X30	W18X35
7	Column 5-6S	W10X 33	W16X26	W16X26	W16X26	W16X26	W14X22
8	Column 7-8S	W8X 18	W12X16	W12X14	W12X14	W12X19	W12X14
Weight (kN)		41.02	32.83	31.68	31.05	31.73	30.98

Note: S = story

The structure's 168 elements are grouped as follows: the same beam section is used in the first and third bay on all floors except for the roof, the beams of the second bay share the same section on all floors except for the roof, the first and third bay beams on the roof share the same section, the beam of the second bay on the roof is an independent variable. This results in 4 beam groups. The exterior columns are combined into one group and the interior columns are combined into another group over three consecutive stories beginning from the foundation. This results in 16 column section groups.

The effective length factor of the members are calculated as $K_x \geq 1$ for a sway-permitted frame and the out-of-plan effective length factors are considered as $K_y = 1$. All of the members are assumed to be unbraced along their lengths.

Two different optimization cases are considered here. In Case 1 the beam sections can be selected from the entire list of W-shapes while the columns are restricted to W14 sections. In Case 2 all the elements are free to be chosen from the entire list of W-shapes.

According to Table 9, the present algorithm finds the best results in both cases. It is also seen that the MCSS performs better than the standard CSS for the cases considered in Kaveh and Talatahari [42].

Fig. 9 and Fig. 10 show the convergence curves of the best runs of MCSS for the 3-bay 24-story frame structure in Case 1 and Case 2, respectively. Fig. 11 and Fig. 12 represent the stress ratios for the members of the 3-bay 24-story frame in Case 1 and Case 2, respectively. Fig. 13 depicts the inter-story drift of the optimal structures in Cases 1 and 2.

5 Concluding remarks

A newly proposed meta-heuristic algorithm named Magnetic Charged System Search Kaveh *et al.* [20], which can be considered as an extension of the standard CSS proposed by Kaveh and Talatahari [19], is utilized here for optimal design of truss and frame structures.

MCSS maintains some extra information about the search space by introducing additional forces called magnetic forces into the standard CSS. These forces are supposed to portray the improvements of the objective function values of the CPs ignoring their relative excellence among the population.

The MCSS algorithm is applied to four structural examples including trusses and frames with different performance constraints. Comparisons of the obtained results with those available in the literature indicate the superiority of the algorithm in finding optimal solutions in the studied examples. Comparisons show that the MCSS generally performances better than the standard CSS.

Acknowledgement

The first author is grateful to the Iran National Science Foundation for the support.

Tab. 9. Comparison of the optimal structures attained by different researchers for the 3-bay 24-story frame.

Element group no.	AISC W-shapes								
	Element group	Saka and Kameshki [39]	Camp et al. [41]	Degertekin [43]	Kaveh and Talatahari [37]		[42]	Present algorithm	
					Case 1	Case 2	Case 1	Case 1	Case 2
1	Beam 1-23S, Bay 1,3	838X292X194UB	W30X90	W30X90	W30X99	W30X99	W30X90	W27X84	W30X90
2	Beam 24S, Bay 1,3	305X102X25UB	W8X18	W10X22	W16X26	W10X33	W21X50	W14X22	W14X22
3	Beam 1-23S, Bay 2	457X191X82UB	W24X55	W18X40	W18X35	W18X35	W21X48	W21X48	W18X35
4	Beam 24S, Bay 2	305X102X25UB	W8X21	W12X16	W14X22	W16X31	W12X19	W14X22	W14X22
5	Column 1-3S, E	305X102X25UC	W14X145	W14X176	W14X145	W36X170	W14X176	W14X145	W27X102
6	Column 4-6S, E	305X368X129UC	W14X132	W14X176	W14X132	W30X116	W14X145	W14X176	W30X132
7	Column 7-9S, E	305X305X97UC	W14X132	W14X132	W14X120	W30X116	W14X109	W14X109	W30X108
8	Column 10-12S, E	356X368X129UC	W14X132	W14X109	W14X109	W24X62	W14X90	W14X109	W27X84
9	Column 13-15S, E	305X305X97UC	W14X68	W14X82	W14X48	W24X62	W14X74	W14X90	W14X43
10	Column 16-18S, E	203X203X71UC	W14X53	W14X74	W14X48	W18X60	W14X61	W14X43	W18X71
11	Column 19-21S, E	305X305X118UC	W14X43	W14X34	W14X34	W16X36	W14X34	W14X43	W24X55
12	Column 21-24S, E	152X152X23UC	W14X43	W14X22	W14X30	W10X33	W14X34	W14X22	W30X90
13	Column 1-3S, I	305X305X137UC	W14X145	W14X145	W14X159	W24X76	W14X145	W14X145	W24X68
14	Column 4-6S, I	305X305X198UC	W14X145	W14X132	W14X120	W14X74	W14X132	W14X120	W21X62
15	Column 7-9S, I	356X368X202UC	W14X120	W14X109	W14X109	W24X62	W14X109	W14X132	W14X90
16	Column 10-12S, I	356X368X129UC	W14X90	W14X82	W14X99	W24X62	W14X82	W14X90	W16X67
17	Column 13-15S, I	356X368X129UC	W14X90	W14X61	W14X82	W18X46	W14X68	W14X68	W27X114
18	Column 16-18S, I	356X368X153UC	W14X61	W14X48	W14X53	W18X46	W14X43	W14X61	W24X55
19	Column 19-21S, I	203X203X60UC	W14X30	W14X30	W14X38	W18X35	W14X34	W14X26	W24X55
20	Column 21-24S, I	254X254X89UC	W14X26	W14X22	W14X26	W16X31	W14X22	W14X22	W10X12
Weight (kN)		958.75	980.63	955.74	967.33	884.88	945.2	925.64	877.22

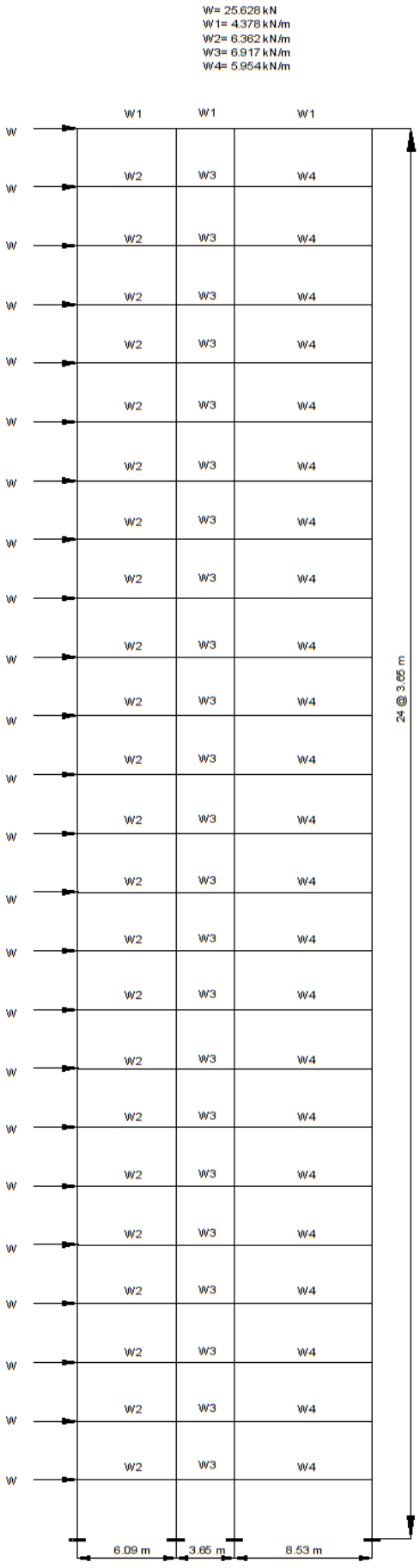

Fig. 8. A 3-bay 24-story frame

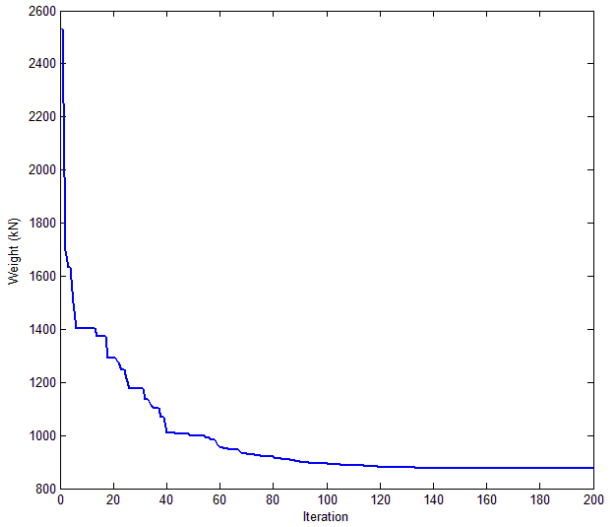

Fig. 9. Convergence curve of the best run for the 3-bay 24-story frame (Case 1)

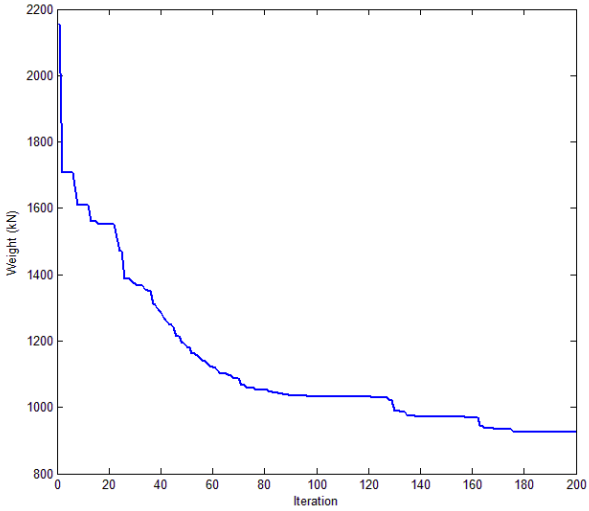

Fig. 10. Convergence curve of the best run for the 3-bay 24-story frame (Case 2)

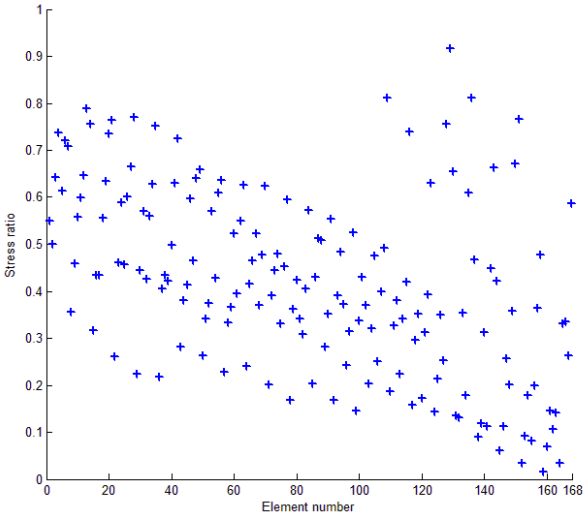

Fig. 11. Stress ratios of the members for the 3-bay 24-story frame (Case 1)

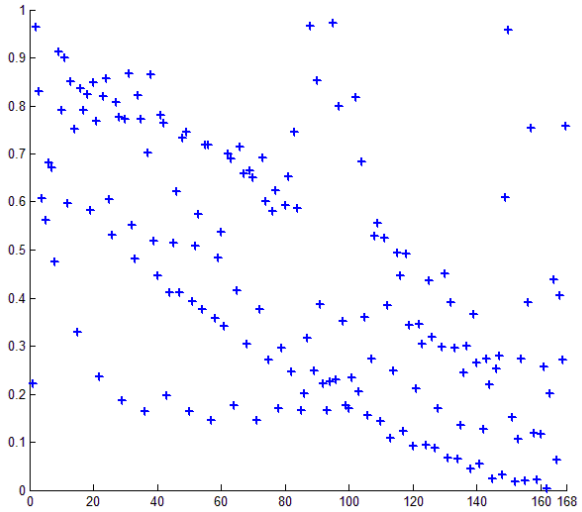

Fig. 12. Stress ratios of the members for the 3-bay 24-story frame (Case 2)

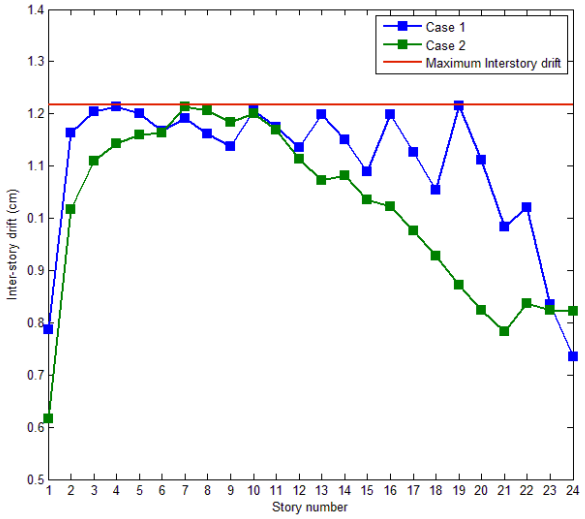

Fig. 13. Inter-story drifts of the optimal structures in Cases 1 and 2

References

1 **Holland J**, *Adaptation in Natural and Artificial Systems*, University of Michigan Press, 1975.

2 **Goldberg D**, *Genetic Algorithms in Search Optimization and Machine Learning*, Addison-Wesley, 1989.

3 **Eberhart R, Kennedy J**, *A new optimizer using particle swarm theory*, Sixth International Symposium on Micro Machine and Human Science, In:, 1995, pp. 39–43.

4 **Dorigo M, Maniezzo V, Colorni A**, *Ant system: optimization by a colony of cooperating agents*, IEEE Transactions on Systems, Man and Cybernetics, Part B (Cybernetics), **26**(1), (1996), 29–41, DOI 10.1109/3477.484436.

5 **Kirkpatrick S, Gelatt C, Vecchi M**, Science, **220**(4598), (1983), 671–680, DOI 10.1126/science.220.4598.671.

6 **Geem Z, Kim J, Loganathan G**, *A New Heuristic Optimization Algorithm: Harmony Search*, Simulation, **76**(2), (2001), 60–68, DOI 10.1177/003754970107600201.

7 **Rashedi E, Nezamabadi-pour H, Saryazdi S**, Information Sciences, **179**(13), (2009), 2232–2248, DOI 10.1016/j.ins.2009.03.004.

8 **Erol O, Eksin I**, *A new optimization method: Big Bang–Big Crunch*, Advances in Engineering Software, **37**(2), (2006), 106–111, DOI 10.1016/j.advengsoft.2005.04.005.

9 **Kaveh A, Talatahari S**, *Size optimization of space trusses using Big Bang–Big Crunch algorithm*, Computers & Structures, **87**(17-18), (2009), 1129–1140, DOI 10.1016/j.compstruc.2009.04.011.

10 **Kaveh A, Laknejadi K, Alinejad B**, *Performance-based multi-objective optimization of large steel structures*, Acta Mechanica, **223**(2), (2012), 355–369, DOI 10.1007/s00707-011-0564-1.

11 **Kaveh A, Talatahari S**, *Charged system search for optimal design of frame structures*, Applied Soft Computing, **12**(1), (2012), 382–393, DOI 10.1016/j.asoc.2011.08.034.

12 **Kaveh A, Talatahari S**, *Particle swarm optimizer, ant colony strategy and harmony search scheme hybridized for optimization of truss structures*, Computers & Structures, **87**(5–6), (2009), 267–283, DOI 10.1016/j.compstruc.2009.01.003.

13 **Kaveh A, Talatahari S**, *Optimization of large-scale truss structures using modified charged system search*, International Journal of Optimization in Civil Engineering, **1**(1), (2011), 15–28.

14 **Kaveh A, Zolghadr A**, *Topology optimization of trusses considering static and dynamic constraints using the CSS*, Applied Soft Computing, **13**(5), (2013), 2727–2734, DOI 10.1016/j.asoc.2012.11.014.

15 **Kaveh A, Zolghadr A**, *Comparison of nine meta-heuristic algorithms for optimal design of truss structures with frequency constraints*, Advances in Engineering Software, **76**, (2014), 9–30, DOI 10.1016/j.advengsoft.2014.05.012.

16 **Kaveh A, Zolghadr A**, *A multi-set charged system search for truss optimization with variables of different natures; element grouping*, Periodica Polytechnica Civil Engineering, **55**(2), (2011), 87–98, DOI 10.3311/pp.ci.2011-2.01.

17 **Csébfalvi A**, *A hybrid meta-heuristic method for continuous engineering optimization*, Periodica Polytechnica Civil Engineering, **53**(2), (2009), 93–100, DOI 10.3311/pp.ci.2009-2.05.

18 **Csébfalvi A**, *Multiple constrained sizing-shaping truss-optimization using ANGEL method*, Periodica Polytechnica Civil Engineering, **55**(1), (2011), 81–86, DOI 10.3311/pp.ci.2011-1.10.

19 **Kaveh A, Talatahari S**, *A novel heuristic optimization method: charged system search*, Acta Mechanica, **213**(3-4), (2010), 267–289, DOI 10.1007/s00707-009-0270-4.

20 **Kaveh A, Motie Share M, Moslehi M**, *Magnetic charged system search: a new meta-heuristic algorithm for optimization*, Acta Mechanica, **224**(1), (2013), 85–107, DOI 10.1007/s00707-012-0745-6.

21 *Manual of steel construction Load resistance factor design*, 3th, American Institute of Steel Construction (AISC); Chicago (IL), 2001.

22 **Dumonteil P**, *Simple equations for effective length factors*, Engineering Journal (AISC), **29**(3), (1992), 111–115.

23 **Grandhi R, Venkayya V**, *Structural optimization with frequency constraints*, AIAA Journal, **26**(7), (1988), 858–866, DOI 10.2514/3.9979.

24 **Sedaghati R, Suleman A, Tabarrok B**, *Structural Optimization with Frequency Constraints Using the Finite Element Force Method*, AIAA Journal, **40**(2), (2002), 382–388, DOI 10.2514/2.1657.

25 **Wang D, Zhang W, Jiang J**, *Truss Optimization on Shape and Sizing with Frequency Constraints*, AIAA Journal, **42**(3), (2004), 622–630, DOI 10.2514/1.1711.

26 **Lingyun W, Mei Z, Guangming W, Guang M**, *Truss optimization on shape and sizing with frequency constraints based on genetic algorithm*, Computational Mechanics, **35**(5), (2005), 361–368, DOI 10.1007/s00466-004-0623-8.

27 **Gomes M**, *Truss optimization with dynamic constraints using a particle swarm algorithm*, Expert Systems with Applications, **38**(1), (2011), 957–968, DOI 10.1016/j.eswa.2010.07.086.

28 **Kaveh A, Zolghadr A**, *Shape and size optimization of truss structures with frequency constraints using enhanced charged system search algorithm*, Asian Journal of Civil Engineering, **12**(4), (2011), 487–509.

29 **Kaveh A, Zolghadr A**, *Truss optimization with natural frequency constraints using a hybridized CSS-BBBC algorithm with trap recognition capability*, Computers & Structures, **102–103**, (2012), 14–27, DOI 10.1016/j.compstruc.2012.03.016.
30 **Wu S, Chow P**, *Steady-state genetic algorithms for discrete optimization of trusses*, Computers & Structures, **56**(6), (1995), 979–991, DOI 10.1016/0045-7949(94)00551-D.
31 **Li L, Huang Z, Liu F**, *A heuristic particle swarm optimization method for truss structures with discrete variables*, Computers & Structures, **87**(7-8), (2009), 435–443, DOI 10.1016/j.compstruc.2009.01.004.
32 **Kaveh A, Talatahari S**, *A particle swarm ant colony optimization for truss structures with discrete variables*, Journal of Constructional Steel Research, **65**(8-9), (2009), 1558–1568, DOI 10.1016/j.jcsr.2009.04.021.
33 *Manual of steel construction allowable stress design*, 9th, American Institute of Steel Construction (AISC); Chicago (IL), 1989.
34 **Khot N, Venkayya V, Berke L**, *Optimum structural design with stability constraints*, International Journal for Numerical Methods in Engineering, **10**(5), (1976), 1097–1114, DOI 10.1002/nme.1620100510.
35 **Camp C, Pezeshk S, Cao G**, *Optimized Design of Two-Dimensional Structures Using a Genetic Algorithm*, Journal of Structural Engineering, **124**(5), (1998), 551–559, DOI 10.1061/(ASCE)0733-9445(1998)124:5(551).
36 **Kaveh A, Shojaee S**, *Optimal design of skeletal structures using ant colony optimization*, International Journal for Numerical Methods in Engineering, **70**(5), (2007), 563–581, DOI 10.1002/nme.1898.
37 **Kaveh A, Talatahari S**, *An improved ant colony optimization for the design of planar steel frames*, Engineering Structures, **32**(3), (2009), 864–873, DOI 10.1016/j.engstruct.2009.12.012.
38 **Davison J, Adams P**, *Stability of braced and unbraced frames*, Journal of Structural Division, ASCE, **100**(2), (1974), 319–334.
39 **Saka M, Kameshki E**, *Optimum design of multi-story sway steel frames to BS 5950 using a genetic algorithm*, Topping BHV, editor, Advances in Engineering Computational Technology, Civil-Camp Press, In:, 1998, pp. 135–141.
40 *British Standards, BS 5950, Structural use of steelworks in building, Part 1 Code of practice for design in simple and continuous construction, hot rolled sections*, British Standard Institution; London, 1990.
41 **Camp C, Bichon J, Stovall S**, *Design of steel frames using ant colony optimization*, Journal of Structural Engineering (ASCE), **131**(3), (2005), 369–379, DOI 10.1061/(ASCE)0733-9445(2005)131:3(369).
42 **Kaveh A, Talatahari S**, *Charged System Search for Optimal Design of Frame Structures*, Applied Soft Computing, **12**(1), (2012), 382–393, DOI 10.1016/j.asoc.2011.08.034.
43 **Degertekin S**, *Optimum design of steel frames using harmony search algorithm*, Structural and Multidisciplinary Optimization, **36**(4), (2008), 393–401, DOI 10.1007/s00158-007-0177-4.